



Study on the Performance of Scroll Compressor Applied for Medium Temperature Refrigeration System

I Nyoman Suamir^{1,*}, I Made Rasta¹, Adi Winarta¹, I Wayan Adi Subagia¹, Made Ery Arsana¹

¹ Department of Mechanical Engineering, Politeknik Negeri Bali, Bukit Jimbaran, Kuta Selatan, Badung, Bali, 80364, Indonesia

ARTICLE INFO

ABSTRACT

Article history:

Received 6 November 2020
Received in revised form 10 May 2021
Accepted 17 May 2021
Available online 16 June 2021

Keywords:

Scroll compressor; medium temperature refrigeration; temperature performance; energy efficiency

Recent research shows great interest in increasing energy efficiency of a refrigeration system and finding appropriate configurations to optimize its performance. One main component in the refrigeration system is compressor. Therefore, the compressor plays an important role in a refrigeration system for energy performance optimization. The study is aimed to experimentally investigate temperature and energy performance of a scroll compressor applied for medium temperature refrigeration systems. Tests were conducted in a water cooled medium temperature refrigeration system. Temperature performance evaluation of the compressor referred to the IEEE Standard 112, while energy efficiency of the compressor was calculated from the energy performance of the refrigeration system. The results clearly show that condensing temperature and evaporating temperature together with degree of superheat at suction gas line can significantly affect temperature performance of a scroll compressor. The results have also shown significant improvement on the overall compressor efficiency accounted for 14% when the evaporating temperature increases from -8.3 °C to -2.4 °C.

1. Introduction

Various steps have been taken to improve energy efficiency and save energy consumption, one of which is the development of compressor technology. One of the most popular types of compressors is scroll compressors [1,2]. Scroll compressors have been applied in various RHVAC applications due to their high efficiency, low noise, low vibration, and low weight compared to other compressor types [3-4]. Scroll compressors are known to be best suited for the refrigerant injection technique, and as a result, extensive research has been carried out on injection scroll compressors [5-7]. Wang *et al.*, [8] performed a numerical simulation to analyze the effect of injection factor on scroll compressor performance. Cho *et al.*, [9] investigated the optimal position and diameter of the injection port for symmetrical and asymmetric scroll compressors. The initial injection shows better performance by increasing the injection mass flowrate. In addition, more injection ports are recommended for asymmetric scroll compressors to compensate for the short injection period. Park *et al.*, [2] conducted a numerical study on a variable speed vapor injection scroll compressor. Vapor

* Corresponding author.

E-mail address: nyomansuamir@pnb.ac.id

<https://doi.org/10.37934/arfmts.83.2.98113>

injection could lower compressor discharge temperatures for all compressor speeds. Qiao *et al.*, [10, 11] developed a transient model of a flash tank vapor injection heat pump considering ambient losses, motor losses, compressor on and off losses.

Scroll compressors are widely used in commercial and residential air conditioning, refrigeration and heat pump applications. For refrigeration, the scroll compressors can be used at high temperature (HT), medium temperature (MT) and even at low temperature (LT). High temperature refrigeration commonly works at evaporating temperature of -3°C up to 1°C and maintaining product temperature in the range between 1°C and 10°C , while MT refrigeration usually operates at evaporating temperature from -10°C to -3°C for keeping product temperature between -1°C and 7°C . Evaporating temperature for LT refrigeration is commonly set below -25°C in order to maintain product temperature lower than -12°C [12]. Application for HT refrigeration for drying has been reported by Ruhyat *et al.*, [13]. MT refrigeration applied for display cabinet can be found in [14] and solar refrigeration system has been reported in [15].

The scroll compressor technology is an orbital motion, positive displacement compressor that compresses refrigerant gas using two spiral-shaped scrolls between snaps. They have no dead space, contact between the sides of the rolls and at the base and top edges is almost perfect and constant; therefore, it has excellent axial and radial suitability. As a result, scroll compressors provide several advantages such as high volumetric efficiency, low vibration and noise, torque variation and low leakage [16-18]. The disadvantage of volumetric compressors is that lubricating oil tends to flow out and mix with the working fluid [19], thereby reducing lubrication capacity, potentially causing engine failure and impacting cycle performance [20]. Hence, there is a clear trend towards oil-free compressors [21,22]. Reducing the power consumption for oil-free compressors is very important as electricity consumption usually accounts for up to 80% of the total compressor life cycle cost [23]. Furthermore, transmission losses can be reduced by replacing large compressors with smaller compressors closer to the end user. The capacity and cooling efficiency of the system decreases with higher condensing temperature and lower evaporation temperature [24-26]. Lower system performance is associated with increased irreversibility during compression, and higher compressor discharge temperatures. This is very important as higher discharge temperatures can result in additional wear on the compressor, reducing reliability and compressor life.

Compressor performance issues arise, often due to heating issues. In fact, an overheated compressor is one of the most common causes of failure. Compressor overheating is the result of internal factors, external conditions or sometimes both. When the compressor gets too hot, the problem is usually related to factors involving irregular suction or discharge pressure. This paper analyses the factors that affect the scroll compressor temperature and energy performance associated with the use of the compressor in MT refrigeration systems. Variation of compressor temperatures including its motor winding temperatures at different condensing and evaporating conditions are comprehensively presented and discussed. Furthermore, effect of the evaporating and condensing temperature as well as degree of superheat to energy efficiency of the compressor is also thoroughly demonstrated and discussed.

2. Methodology

2.1 Test Equipment and Measurement System

The scroll compressor to be tested was a hermetic compressor of a vertical display cabinet which incorporated a built-in condensing unit. The condensing unit was operated as MT refrigeration system and placed at the top part of the display cabinet. Refrigerant R-1270 was used for the cabinet. R-1270 is hydrocarbon refrigerant and classified as an A3 safety group [27,28]. This constrains the

concentration of the refrigerant in a room to be lower than its flammability limit. The refrigeration system of the cabinet was charged within the safety limit as specified in [27].

Detailed schematic of the test system incorporated refrigeration system with scroll compressor and heat rejection system is shown in Figure 1. Refrigeration system of the test system rejected heat to the ambient through water cooled heat exchangers. The heat exchanger was piped to a water heat rejection system which was developed to enable the condensing temperature of the refrigeration system to be accurately controlled. By adjusting T_{set} on the temperature control set, the condensing temperature can indirectly be changed according to the testing needs. This is due to the temperature control set can control temperature of the cooling water by regulating the operation of the electric heater and air cooled chiller as shown in the figure. The cooling water temperature is actually the main control parameter that can directly affect the condensing temperature of the refrigeration system.

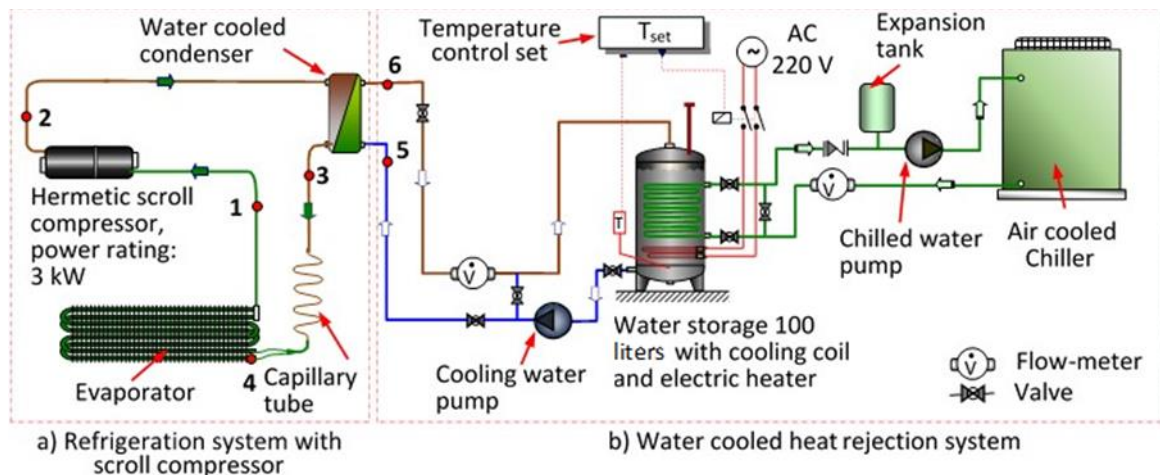


Fig. 1. Schematic diagram of the test system equipped with water circuit heat rejection system and measurement points

The test system is equipped with a measurement system which measures parameters of the compressor and refrigeration systems. The parameters involve refrigerant pressure and temperature, cooling water temperature, power consumption, and mass flowrate. Particularly for the compressor parameters, additional temperature measurement points were added which included suction line, case (body) of the compressor, and discharge line. A set up of measurement was also arranged for testing the resistance of compressor motor windings (main winding and auxiliary winding) according to IEEE Standard 112 [29]. Schematic diagram of the resistance winding measurement can be seen in Figure 2. Points C, S, and R indicate connection terminals of the compressor where the electrical circuit of the refrigeration system to be connected. C is known as common terminal; S is start winding or auxiliary winding terminal; and R is run winding or main winding terminal. Before measurement, all connections from compressor motor terminals to the electrical circuit are disconnected. While detailed instruments used in the test system are listed in Table 1. For data acquisition and recording, a computer set was also set up to complete the measurement system.

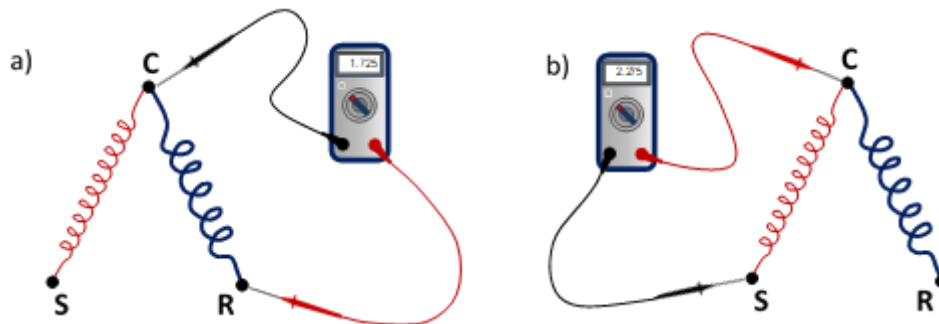


Fig. 2. Resistance measurement of the compressor motor windings: a) Measurement for main winding; b) auxiliary winding measurement

Table 1

The instruments used in the test system completed with their type, accuracy, range and number

Instruments	Type	Accuracy	Range	Number
Temperature sensors	T type thermocouple	$\pm 0.5^{\circ}\text{C}$	-250 to 350 $^{\circ}\text{C}$	12
LP Pressure transducers	Piezoelectric 0-10 V	$\pm 0.8\%$	-1 to 9 bar	2
HP Pressure transducers	Piezoelectric 0-10 V	$\pm 0.8\%$	1 to 24 bar	2
Flow meter	Electromagnetic-IFC010D	$\pm 0.3\%$	0.5 to 21 m^3h^{-1}	2
Multi meter	Digital, 87V Max	$\pm(0.2\% + 1)$	0.1 Ω to 50 $\text{M}\Omega$	1
Power meter	Digital power analyzer, HM8115-2	$\pm 0.8\%$	0.001 W to 8 kW	1
DataScan processor and expansion module	7320 series and 7020 series	$\pm 0.02\%$ rdgs + 0.01% range	16 bits@40 rdgs/sec 14 bits@400 rdgs/sec	1

Note: LP = low pressure range; HP = high pressure range; rdgs = readings

2.2 Test Conditions

The scroll compressor was tested in MT refrigeration test conditions. Two test conditions were performed. First test condition was conducted at evaporating pressure (P_{evap}) and temperature (T_{evap}) to be maintained constant at 4.8 bar and -0.6°C respectively. While the condensing pressure (P_{cond}) and temperature (T_{cond}) were gradually increased from 12.8 bar to 14.9 bar and 32.5°C to 38.5°C respectively as shown in Table 2.

Table 2

Pressure and saturated temperature for the first test conditions

Pressure		Temperature	
P_{cond} (bar)	P_{evap} (bar)	T_{cond} ($^{\circ}\text{C}$)	T_{evap} ($^{\circ}\text{C}$)
12.8	4.8	32.5	-0.6
13.2	4.8	33.5	-0.6
13.5	4.8	34.5	-0.6
13.8	4.8	35.0	-0.6
14.0	4.8	35.5	-0.6
14.4	4.8	36.5	-0.6
14.9	4.8	38.5	-0.6

Investigation on the compressor temperature and performance was carried out at different condensing temperature. The investigation was based on resistance measurement of the compressor motor windings. Data from the compressor windings was recorded at every increment of the

condensing temperature. The winding resistance measurement was conducted within 30 second after the refrigeration system was shut off. Before shutting down, the refrigeration system was steadily operated for about 4 hours as indicated in IEEE Standard 112.

The second test was carried out at different evaporating temperatures. The evaporating temperatures were gradually increased from -8.3 °C to -5.1 °C by increasing cooling load of the display cabinet. While the cooling load can be altered through regulation of the test chamber temperature. The evaporating temperature range corresponded to the saturation pressure from 3.5 bar to 4.0 bar as can be seen in Table 3. In this test the condensing temperature and pressure of the refrigeration system respectively increased from 28.9 °C to 30.3 °C and 11.7 bar to 12.2 bar. The increase was mainly due to the increase of evaporator load.

Table 3
 Pressure and saturated temperature for the
 second test conditions

Pressure		Temperature	
P _{cond} (bar)	P _{evap} (bar)	T _{cond} (°C)	T _{evap} (°C)
11.69	3.53	28.9	-8.3
11.76	3.59	29.1	-7.9
11.82	3.66	29.3	-7.5
11.88	3.68	29.5	-7.1
11.94	3.76	29.7	-6.6
11.94	3.80	29.7	-6.3
11.97	3.91	29.8	-5.6
12.04	4.13	30.0	-4.2
12.10	4.31	30.2	-3.1
12.13	4.42	30.3	-2.4

The compressor temperature and performance were investigated at different evaporating temperatures. Winding temperature was also estimated by using the resistance of the windings and was also measured according to IEEE Standard 112 at every increment of the evaporating temperature as shown in Table 3.

2.3 Methods

Refrigeration system of the display cabinet, where the scroll compressor to be installed, was tested according to [12]. Operational data of the refrigeration system was recorded every 10 seconds in order to comply with the standard which included pressure and temperature of the refrigerant at four points of measurement, cooling water temperature, power consumption and cooling water mass flowrate. The measurement points are shown in Figure 1. While the average temperature of the compressor motor windings was determined according to IEEE Standard 112.

$$T_{main} = \frac{R_{main}}{R_{cold}} (234.5 + T_{cold}) - 234.5 \quad (°C) \quad (1)$$

$$T_{aux} = \frac{R_{aux}}{R_{cold}} (234.5 + T_{cold}) - 234.5 \quad (°C) \quad (2)$$

where, T_{main} is the temperature of main winding during the test when R_{main} is measured ($^{\circ}C$); T_{aux} is the temperature of auxiliary winding during the test when R_{aux} is measured ($^{\circ}C$); R_{main} is the main winding resistance measured (ohms); R_{aux} is the auxiliary winding resistance measured (ohms); R_{cold} is the known value of winding resistance at temperature T_{cold} (ohms); T_{cold} is the temperature of winding when known value of resistance R_{cold} is measured ($^{\circ}C$); 234.5 is a constant for 100% IACS (International Annealed Copper Standard) conductivity copper, or 225 for aluminum, based on a volume conductivity of 62%.

The winding resistances were measured after the refrigeration system was shutdown. The winding resistances were obtained within the time indicated in IEEE Standard 112. For an electric motor rating 3 kW which is lower than 38 kW, time interval after switching off the power is within 30 seconds. In this study, for known-value winding resistance (R_{cold}) was investigated at temperature $T_{cold} = 27.4^{\circ}C$. Measurement results are presented in Table 4.

Table 4
 Measurement results on the reference resistance of the compressor motor windings

Parameters	Main winding	Auxiliary winding
Cold temperature (T_{cold}) in $^{\circ}C$	27.4	27.4
Cold resistance (R_{cold}) in ohms	1.725	2.275

The data obtained from the measurement system were processed in a spreadsheet software and simulated in EES (Engineering Equation Solver) program. EES program was used to retrieve thermodynamic properties of the refrigerant R-1270 and cooling water as well as to evaluate compressor efficiencies at different test conditions. Energy of the refrigeration system was analyzed according to the first law of thermodynamics. Some assumptions were also applied such as: insignificant pressure loss in the system, isenthalpic-expansion process in the capillary tube of the refrigeration system and negligible heat loss in the water cooled condenser.

Mass flowrate of the refrigerant (\dot{m}_r) through the compressor is determined by using energy balance in the water-cooled condenser as shown in Eq. (3) (parameter numbers refer to Figure 1).

$$\dot{m}_r = \frac{\dot{m}_w C_p (T_6 - T_5)}{h_2 - h_3} \quad (\text{kg s}^{-1}) \quad (3)$$

where, \dot{m}_w = water mass flowrate (kg s^{-1}); C_p = specific heat capacity of cooling water ($\text{kJ kg}^{-1} \text{ }^{\circ}C^{-1}$); T_5 and T_6 = entering and leaving temperature of cooling water at the condenser ($^{\circ}C$); h_2 and h_3 = entering and leaving specific enthalpy of refrigerant at the condenser (kJ kg^{-1}).

Isentropic efficiency (η_s) of the scroll compressor can be calculated from specific isentropic compression work divided by specific hydraulic compression work as can be seen in Eq. (4). The overall efficiency of the compressor (η_{comp}) is determined from the ratio of isentropic compression work ($\dot{m}_r (h_{2s} - h_1)$) and compressor power (W_{comp}) as shown in Eq. (5).

$$\eta_s = \frac{h_{2s} - h_1}{h_2 - h_1} \times 100 \% \quad (\%) \quad (4)$$

$$\eta_{comp} = \frac{\dot{m}_r (h_{2s} - h_1)}{W_{comp}} \times 100\% \quad (\%) \quad (5)$$

where, \dot{m}_r = refrigerant mass flowrate (kg s^{-1}); h_1 = specific enthalpy of refrigerant at suction line of the compressor (kJ kg^{-1}); h_2 = specific enthalpy of refrigerant at discharge line of the compressor (kJ kg^{-1}); h_{2s} = specific enthalpy of refrigerant at discharge line which has the same entropy as the suction line (kJ kg^{-1}); W_{comp} = electrical power consumption of the scroll compressor (kW).

Ratio between overall efficiency of the compressor (η_{comp}) and adiabatic efficiency (η_1) can also be written as hydraulic compression work divided by compressor's electrical power as shown in Eq. (6). This ratio is expressed as η_2 and it can be used to indicate compressor's motor efficiency [31].

$$\eta_2 = \frac{\eta_{comp}}{\eta_1} = \frac{\dot{m}_r (h_2 - h_1)}{W_{comp}} \times 100\% \quad (\%) \quad (6)$$

where, overall efficiency of the compressor is defined as Eq. (7) [31] and adiabatic efficiency of the compressor (η_1) is expressed as theoretical adiabatic (isentropic) compression work divided by hydraulic compression work:

$$\eta_{comp} = \eta_1 \eta_2 \quad (7)$$

$$\eta_1 = \frac{\dot{m}_r (h_{2s} - h_1)}{\dot{m}_r (h_2 - h_1)} \times 100\% \quad (\%) \quad (8)$$

3. Results and Discussion

3.1 Temperature Performance at Different Condensing Temperatures

Testing on the scroll compressor at varied condensing temperatures has been performed. The compressor temperatures involving suction, case (body) and discharge temperatures have been measured and recorded. Test conditions were as described in Table 2. Degree of superheat refrigerant exiting evaporator was recorded ranging from 10 to 12 °C. Variation of the compressor temperatures at different condensing temperatures can be seen in Figure 3. Temperature of the suction line of the compressor somewhat increases as high as 1.9 °C when the condensing temperature increases from 32.5 to 38.5 °C. Condensing temperature has a low impact on the temperature of the compressor suction line. This is commonly caused by cooling effect of refrigerant flowing from the evaporator which has relatively lower temperature. Temperature rise at suction line predominantly caused by evaporator loading system. When evaporator cooling load goes up at the same evaporating temperature, it can rise degree of superheat of the refrigerant leaving the evaporator. This superheat then increases the suction line temperature of the compressor. The result indicates degree of superheat at suction line can also boost temperatures of body and discharge line of the compressor.

The temperatures of body and discharge area, however, show a considerable increase of about 7.6 °C accounted for 26.7 % higher than the increase of condensing temperature. This occurs as the result of compression process. Energy used to compress the superheated refrigerant vapor turns into heat and rises the refrigerant temperature, pressure and enthalpy. The refrigerant state exits the compressor is superheated gas. Some heat also dissipates to the body of the compressor and some lose to the surrounding air. The compression temperature in the compressor is practically always

higher than the condensing temperature. Therefore, some heat is rejected out from the refrigeration system at temperatures above the condensing temperature which is known as de-superheated process. This result signifies a deviation from the ideal refrigeration cycle.

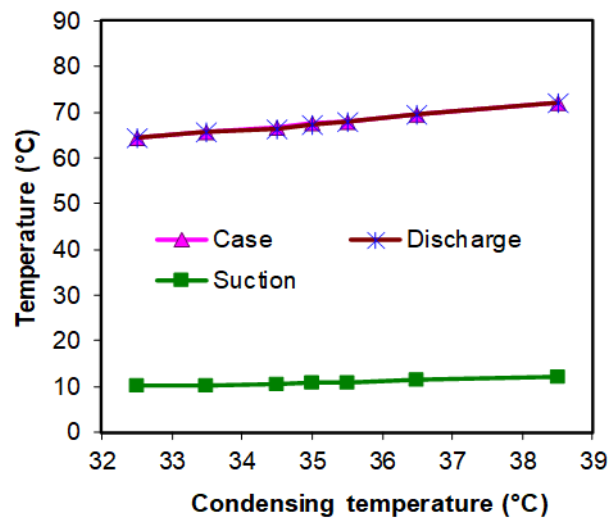


Fig. 3. Temperature variation of case (body), suction and discharge line

Figure 4 shows variation of compressor motor winding temperatures at different temperatures of condensation. From the graph, it can be seen that the motor winding temperatures proportionally increase with the condensing temperature. When the condensing temperatures change from 32.5 to 38.5 °C, temperatures of main and auxiliary windings increase for about 6.0 °C and 5.7 °C respectively. Temperatures of motor windings illustrated in Figure 4 were calculated from Eq. (1) and Eq. (2) based on measured resistances as presented in Table 5. The winding resistances and temperatures rise when the condensing temperature increases.

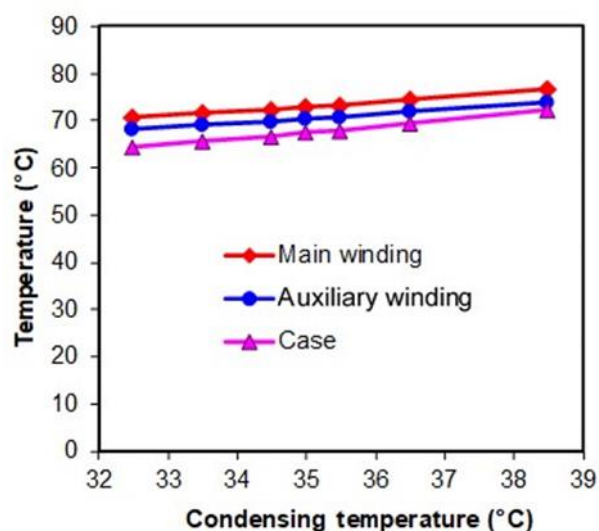


Fig. 4. Winding temperatures of the scroll compressor motor at different condensing temperatures

For the first test conditions, it has been found that temperature of main winding (T_{main}) and auxiliary winding (T_{aux}) to be higher than the compressor body (case) temperature. This is essentially reasonable because the motor windings generate heat due to inefficient energy conversion from electrical to mechanical energy. Inefficiency of standard electric motor with power rating 3 kW can reach 15% [30]. To reach this level of temperatures, the motor windings have actually been assisted by refrigerant cooling from the suction line of the compressor. Within a hermetic scroll compressor, refrigerant from suction line is circulated through the motor windings by which can reduce their temperature and prevent them from overheating.

Table 5

The resistance and temperature of compressor motor windings at various condensing temperatures

T_{cond} (°C)	Motor windings			
	R_{main} (Ohms)	T_{main} (°C)	R_{aux} (Ohms)	T_{aux} (°C)
32.5	2.01	70.7	2.63	68.3
33.5	2.02	71.6	2.64	69.2
34.5	2.02	72.3	2.64	69.8
35.0	2.03	73.0	2.65	70.5
35.5	2.03	73.4	2.65	70.9
36.5	2.04	74.6	2.66	72.0
38.5	2.05	76.7	2.68	74.0

R_{main} = main winding resistance; R_{aux} = auxiliary winding resistance; T_{main} = main winding temperature; T_{aux} = auxiliary winding temperature

3.2 Temperature Performance at Varied Evaporating Temperatures

Temperature performance of the scroll compressor at various evaporating temperatures has also been tested and analyzed. Variation of suction, case (body) and discharge temperatures at different evaporation temperatures are illustrated in Figure 5.

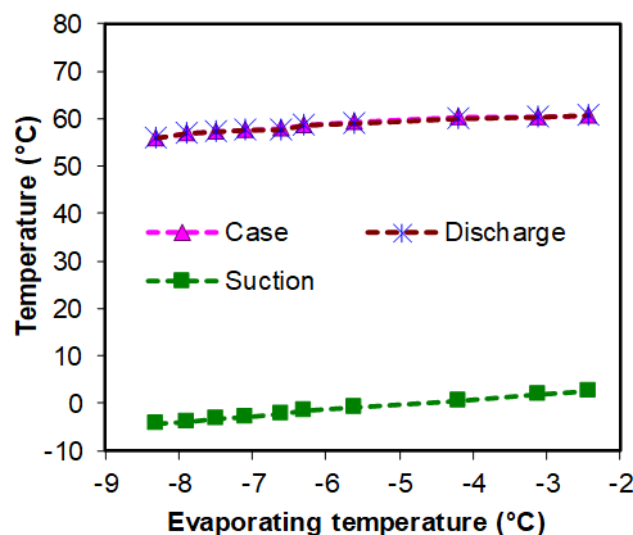


Fig. 5. Temperature variation of the case, suction and discharge line at different evaporating temperatures

Condensing temperature was maintained relatively constant with small variation from about 29 to 30 °C. From the graph, it can be seen temperature of the suction line of the compressor increases from -4.3 °C to 2.6 °C with degree of superheat in the range between 4 and 5 °C. The results also show that temperatures of body compressor and discharge line are nearly the same which both increase from 56 to 60.5 °C. This indicates that evaporating temperature can positively affect temperature of the compressor body and discharge line. With the same degree of superheat of about 5 °C, body and discharge line temperatures of the scroll compressor increase when the evaporating temperature increases. It is also found that suction line temperature rises when degree of superheat refrigerant leaving the evaporator increases. The higher degree of superheat refrigerant exiting the evaporator, the higher the suction line temperature. This can significantly increase temperature of the compressor and discharge line.

Disparity of compressor winding temperatures at different evaporating temperatures is shown in Figure 6. The graph also shows motor winding temperatures proportionally increase with evaporating temperature. Temperatures of main and auxiliary windings increase for about 4.6 °C when the evaporating temperature rises from -8.3 to -2.4 °C. Temperatures of motor windings shown in Figure 6 were also determined using Eq. (1) and Eq. (2). The calculation was based on resistances of the windings at correlated evaporating temperatures as presented in Table 6. The winding resistance rises when the compressor operated at higher evaporation temperature. This also indicates the increase of the motor windings temperature.

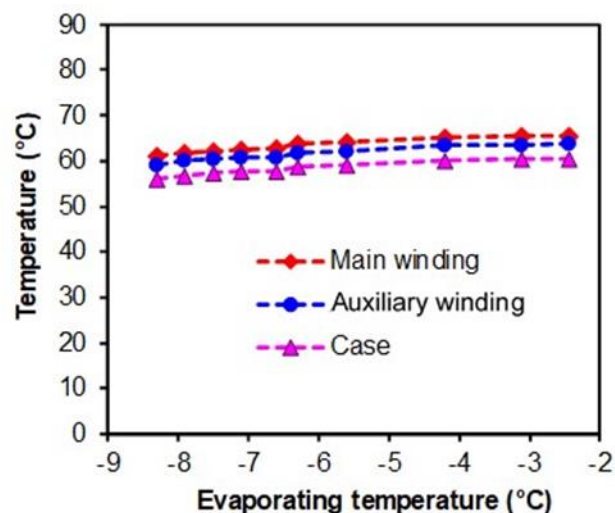


Fig. 6. Winding temperatures of the compressor motor at varied evaporating temperatures

On the second test with evaporating temperature variation, it has also been found that temperature of main winding (T_{main}) is about 2 °C higher than the auxiliary winding (T_{aux}). Both winding temperatures are higher than the compressor body (case) temperature. Main winding and auxiliary winding of the compressor motor are found 7 °C and 5 °C to be respectively hotter than compressor body temperature. This is logical because the motor windings generate heat due to inefficiency energy conversion as discussed previously. With lower evaporating temperature the motor windings can operate as low as 61 °C for evaporating temperature of -8.3 °C (Table 6) and significantly increase to 76.7 °C when the evaporating temperature rises to -0.6 °C (Table 3 and Table 6). This is also simultaneously caused by the increase of superheat at suction line of the compressor which changes from 5 °C to 12 °C. The study results clearly indicate that evaporating temperature

together with degree of superheat at suction line of the compressor can significantly affect temperature performance of the scroll compressor.

Table 6

The resistance and temperature of motor windings at different evaporating temperatures

T _{evap} (°C)	Motor windings			
	R _{main} (Ohms)	T _{main} (°C)	R _{aux} (Ohms)	T _{aux} (°C)
-8.3	1.95	61.0	2.55	59.1
-7.9	1.95	61.9	2.56	60.0
-7.5	1.95	62.3	2.56	60.4
-7.1	1.96	62.6	2.56	60.7
-6.6	1.96	62.8	2.57	60.9
-6.3	1.96	63.7	2.57	61.8
-5.6	1.97	64.1	2.58	62.2
-4.2	1.97	65.3	2.59	63.4
-3.1	1.98	65.5	2.59	63.6
-2.4	1.98	65.6	2.59	63.7

3.3 Energy Performance Analysis

In this study energy performance of the compressor is analyzed which include isentropic (η_s) and overall compressor efficiencies (η_{comp}). Compressor efficiencies have been determined for varied condensing and evaporating temperatures by using Eq. (4) and Eq. (5). The results at different condensing temperature are illustrated in Figure 7. The figure shows a fairly constant refrigerant mass flowrate of 0.03 kg/s. However, both isentropic and overall compressor efficiencies seem to be slightly reduced, if not constant, of about 66,1% and 51,7% respectively. The overall compressor efficiency is 14.3% lower than the isentropic efficiency. Motor efficiency (η_2) of the compressor calculated from Eq. (6) is 78,3%. This means inefficiency of the compressor motor is about 21.7%. The inefficiency is higher than that of a standard motor as stated in [30].

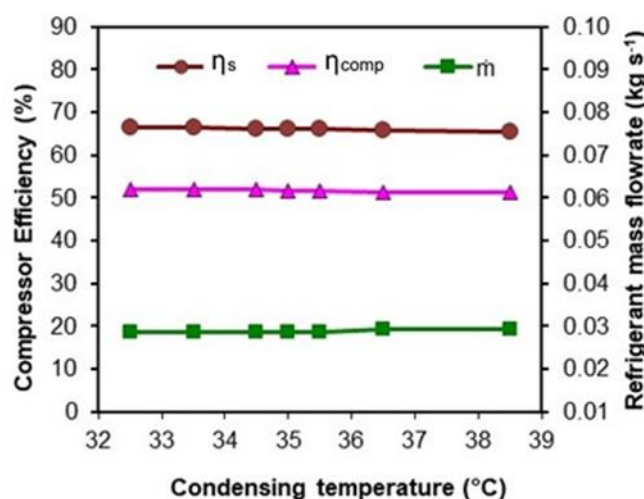


Fig. 7. Scroll compressor efficiencies and refrigerant mass flowrate at different condensing temperatures

Interesting results are found on the test with varied evaporating temperatures as it can be seen in Figure 8. Isentropic efficiency is slightly increase for about 2% with average of 64.2% when the evaporating temperature changes from $-8.3\text{ }^{\circ}\text{C}$ to $-2.4\text{ }^{\circ}\text{C}$. Overall efficiency of the compressor, however, is lower than isentropic efficiency and it is found to increase from 45.1% to 51.4% accounted for an increase of 14%. This also means that overall efficiency of the compressor increases when the compression ratio decreases as shown in Table 7.

Figure 8 also shows increase of the refrigerant mass flowrate. When evaporating temperature varies from $-8.3\text{ }^{\circ}\text{C}$ to $-2.4\text{ }^{\circ}\text{C}$, the mass flowrate increases from 0.025 kg s^{-1} to 0.03 kg s^{-1} accounted for about 22.5%. By using Eq. (6), compressor's motor efficiency can also be determined which ranges from 71.6% to 79.1%. The efficiency also increases with evaporating temperature. Inefficiency of the compressor motor at varied evaporating temperatures is also higher than that of a standard motor.

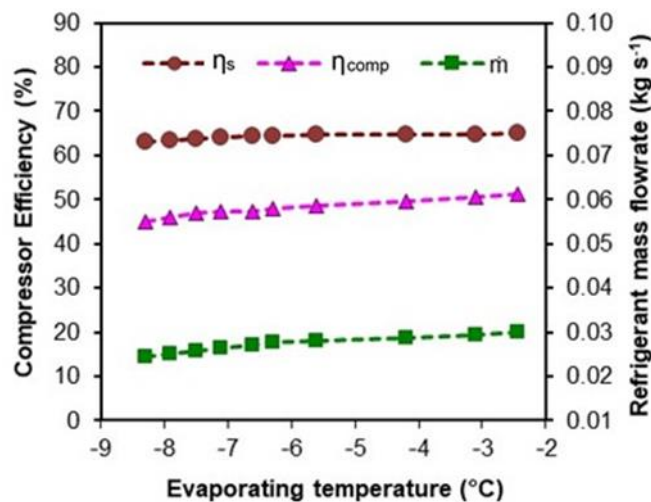


Fig. 8. Scroll compressor efficiencies and refrigerant mass flowrate at varied evaporating temperatures

Density of refrigerant gas at suction compressor was also determined based on data of pressure and temperature obtained from the tests. Figure 9 shows variation of the suction gas density investigated at various evaporating and condensing temperatures. Density of suction gas gradually rises when evaporating temperature increases. The suction gas density at different condensing temperatures (where the evaporating temperature was maintained fairly stable at $-0.6\text{ }^{\circ}\text{C}$) was found to be relatively constant of 9.34 kg m^{-3} . There is a little changed, as shown in Figure 9, due to different degree of superheat (Table 7). This verifies test results that show an increase in the refrigerant mass flowrate in a fixed speed compressor when the evaporating temperature increases (Figure 8).

Test results show the tested compressor has low isentropic efficiency ranging from 63% to 66.4%. According to Rosen *et al.*, [32], isentropic efficiencies of a compressor vary from 65% to 100% for the low to high efficiency respectively. The compressor's motor efficiency is also found lower than that of standard motor with inefficiency more than 15%. These low efficiencies subsequently result in low overall compressor efficiency. These are possibly due to the refrigeration system has new and unique structure of implementing environmentally friendly refrigerant R-1270 for a display cabinet. Some components were found to have capacity that did not meet the specified specifications. In addition of that, the display cabinet was being tested for system optimization.

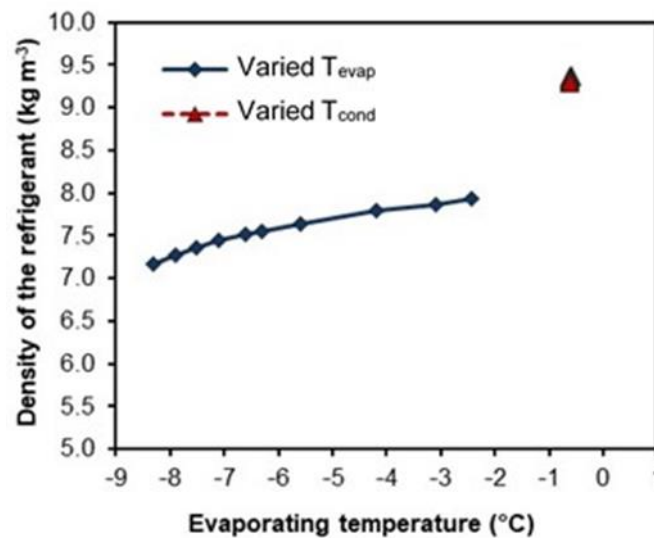


Fig. 9. Density of suction gas refrigerant at different evaporating and condensing temperatures

Table 7

Energy performance parameters of the scroll compressor at different condensing and evaporating temperatures

T_{evap} (°C)	T_{cond} (°C)	ΔT_{sh} (°C)	Pressure ratio	W_{comp} (kW)	η_s (%)	η_2 (%)	η_{comp} (%)	T_{disch} (°C)
<i>Investigated at varied condensing temperature</i>								
-0.6	32.5	10.7	2.67	2.80	66.4	78.5	52.1	64.5
-0.6	33.5	10.8	2.75	2.82	66.4	78.5	52.1	65.7
-0.6	34.5	11.1	2.81	2.83	66.2	78.3	51.8	66.5
-0.6	35.0	11.4	2.88	2.84	66.1	78.3	51.8	67.4
-0.6	35.5	11.6	2.92	2.85	66.0	78.2	51.6	68.0
-0.6	36.5	12.1	3.00	2.86	65.8	78.2	51.4	69.5
-0.6	38.5	12.6	3.10	2.88	65.6	78.2	51.3	72.1
<i>Investigated at varied evaporating temperature</i>								
-8.3	28.9	4.00	3.31	2.77	63.0	71.6	45.1	55.9
-7.9	29.1	4.10	3.28	2.78	63.3	72.8	46.1	56.8
-7.5	29.3	4.20	3.23	2.79	63.7	73.9	47.0	57.2
-7.1	29.5	4.30	3.24	2.80	64.0	74.0	47.3	57.5
-6.6	29.7	4.50	3.19	2.82	64.3	73.7	47.4	57.7
-6.3	29.7	4.60	3.15	2.83	64.5	74.5	48.1	58.6
-5.6	29.8	4.70	3.07	2.84	64.6	75.5	48.8	59.0
-4.2	30.0	4.80	2.93	2.85	64.7	76.6	49.5	60.2
-3.1	30.2	4.90	2.81	2.86	64.9	78.0	50.6	60.4
-2.4	30.3	5.00	2.75	2.88	65.0	79.1	51.4	60.5

ΔT_{sh} = degree of superheat of suction gas; T_{disch} = discharge line temperature; η_s = isentropic efficiency; η_2 = motor efficiency; η_{comp} = overall efficiency

The results also show energy efficiency of the scroll compressor for medium temperature refrigeration application is very much influenced by evaporating temperature. The condensing temperature has less effect on the energy performance. Energy efficiency of the compressor can significantly improve when the refrigeration system to be operated at higher evaporating temperature. As shown in Table 7, compressor efficiencies including motor efficiency increase when the evaporating temperature rises from -8.3 °C up to -2.4 °C. On the other hand, even though the

condensing temperature is changed from 32.5 °C to 38.5 °C, the compressor efficiencies are relatively unchanged when the evaporating temperature is kept constant.

Evaporating and condensing temperatures together with degree of superheat of suction gas are found to significantly affect temperature of the compressor which include temperatures of body compressor, discharge line and motor windings. Higher evaporating temperature, condensing temperature and degree of superheat can considerably boost temperatures of the compressor. These three variables can increase temperature of the compressor (indicated from discharge gas line temperature) of about 16 °C. However, condensing temperature has low impact on the temperature of the suction area of the compressor. This is caused by cooling effect from refrigerant flowing from the evaporator which has relatively lower temperature.

These findings strengthen results of mostly published researches in refrigeration field which have stated significant improvement of system COP (coefficient of performance) when a refrigeration system is operated at higher evaporating temperature. Higher evaporating temperature can increase refrigeration capacity; lower power consumption and improve compressor efficiency as it has been found and proven in this study. Additionally, the results are also in agreement with [24-26] who have reported that capacity and cooling efficiency of a refrigeration system decreases with higher condensing temperature and lower evaporating temperature.

4. Conclusions

Testing of the scroll compressor at varied condensing and evaporating temperatures for medium temperature refrigeration application has been performed. Temperature performance of the scroll compressor at various evaporating temperatures shows that evaporating temperature can affect temperature of the compressor body and discharge line. Body and discharge line temperatures of the scroll compressor increase when the evaporating temperature increases. It is also found that higher condensing temperature can significantly increase temperature of the compressor and discharge line. This study has clearly indicated that condensing temperature and evaporating temperature together with degree of superheat at suction gas line of the compressor can substantially affect temperature performance of the scroll compressor. Additionally, evaporating temperature has also been proved that it can considerably influence efficiencies of the scroll compressor applied for medium temperature refrigeration system.

Acknowledgement

The research associated with this paper was financially supported by the Higher Education Directorate General of the Ministry of Research, Technology and Higher Education (RTHE) of the Republic of Indonesia under international collaboration with Brunel University London and Bali State Polytechnic. The authors would like to thank Ministry of RTHE for the financial support and Bali State Polytechnic (Politeknik Negeri Bali) as well as Brunel University for the research facility.

References

- [1] Zendejboudi, A. and A. Tatar. "Oil flooded scroll compressors: Predicting the energy performance and evaluating the experimental data, measurement." *Measurement* 112 (2017): 38-46. <https://doi.org/10.1016/j.measurement.2017.08.011>
- [2] Park, Y., Y. Kim, H. Cho. "Thermodynamic analysis on the performance of a variable speed scroll compressor with refrigerant injection." *Int. J. Refrig.* 25 (2002): 1072-82. [https://doi.org/10.1016/S0140-7007\(02\)00007-5](https://doi.org/10.1016/S0140-7007(02)00007-5)
- [3] Laughman, C.R., P.R. Armstrong, L.K. Norford, S.B. Leeb. "The Detection of Liquid Slugging Phenomena in Reciprocating Compressors via Power Measurements." *International Compressor Engineering Conference*, C084. (2006): 1-8.

- [4] Qin, F., G. Zhang, Q. Xue, H. Zou, C. Tian. "Experimental investigation and theoretical analysis of heat pump systems with two different injection portholes compressors for electric vehicles." *Appl. Energy* 185 (2017): 2085-93. <https://doi.org/10.1016/j.apenergy.2015.12.032>
- [5] Zehnder, M., D. Favrat, H. Hohl, M. Perevozchikov. "High performance air-water heat pump with extended application range for residential heating." *Seventh int. energy agency conf. heat. pump. technol.* (2017): 19-22.
- [6] Winandy, E.L. and J. Lebrun. "Scroll compressors using gas and liquid injection: experimental analysis and modelling." *Int. J. Refrig.* 25 (2002): 1143-56. [https://doi.org/10.1016/S0140-7007\(02\)00003-8](https://doi.org/10.1016/S0140-7007(02)00003-8)
- [7] Guoyuan, M., C. Qinhu, J. Yi. "Experimental investigation of air-source heat pump for cold regions." *Int. J. Refrig.* 26 (2003): 12-18. [https://doi.org/10.1016/S0140-7007\(02\)00083-X](https://doi.org/10.1016/S0140-7007(02)00083-X)
- [8] Wang, B., W. Shi, X. Li. "Numerical analysis on the effects of refrigerant injection on the scroll compressor." *Appl. Therm. Eng.* 29 (2009): 37-46. <https://doi.org/10.1016/j.applthermaleng.2008.01.025>
- [9] Cho, I.Y., S.B. Ko, Y. Kim. "Optimization of injection holes in symmetric and asymmetric scroll compressors with vapor injection." *Int. J. Refrig.* 35 (2012): 850-60. <https://doi.org/10.1016/j.ijrefrig.2012.01.007>
- [10] Qiao, H., V. Aute, R. Radermacher. "Transient modeling of a flash tank vapor injection heat pump system - Part I: model development." *Int. J. Refrig.* 49 (2015): 169-82. <https://doi.org/10.1016/j.ijrefrig.2014.06.019>
- [11] Qiao, H., X. Xu, V. Aute, R. Radermacher. "Transient modeling of a flash tank vapor injection heat pump system - Part II: simulation results and experimental validation." *Int. J. Refrig.* 49 (2015): 183-94. <https://doi.org/10.1016/j.ijrefrig.2014.06.018>
- [12] BS EN ISO 23953-2 +A1. (2012). *Refrigerated display cabinets; Part 2: Classification, requirements, and test conditions.* The British Standards Limited, UK.
- [13] Ruhyat, N., E.A. Kosasih, Warjito, I.H. Imansyah. "Combination system of spray dryer and low evaporator temperature refrigeration for drying vitamine B1." *Journal of Advanced Research in Fluid Mechanics and Thermal Sciences* 55 (2019): 102-110.
- [14] Suamir, I.N., M.E. Arsana, K.M. Tsamos. "Experimental Study on the Influences of Air Flow in an Integral Hydrocarbon Display Cabinet to its Temperature and Energy Performances." *IOP Conf. Ser.: Mater. Sci. Eng.* 494 (2019): 012017. <https://doi.org/10.1088/1757-899X/494/1/012017>
- [15] Jamaluddin, M.S., M.M. Rahman, M.F. Hasan, A. Saat, M.A. Wahid. "Performance evaluation of a small-scale solar driven refrigeration system." *Journal of Advanced Research in Fluid Mechanics and Thermal Sciences* 55 (2019): 102-110.
- [16] Sun, S., X. Wang, P. Guo, Z. Song. "Investigation on the modifications of the suction flow passage in a scroll refrigeration compressor." *Appl. Ther. Eng.* (2020): 115031. <https://doi.org/10.1016/j.applthermaleng.2020.115031>
- [17] ASHRAE Handbook. (2019). *HVAC Systems and Equipment.* American Society of Heating, Refrigerating and Air-Conditioning Engineers, Inc., Atlanta, USA.
- [18] Fernando, M., T. Oquendo, E.N. Peris, F.B. Ruescas, J.G. Macía. "Semi-empirical model of scroll compressors and its extension to describe vapor-injection compressors: Model description and experimental validation." *Int. J. Refrig.* 106 (2019): 308-326. <https://doi.org/10.1016/j.ijrefrig.2019.06.031>
- [19] Nordtvedt, S.R. (2005). *Experimental and theoretical study of a compression/absorption heat pump with ammonia/water as working fluid.*
- [20] Demierre, J., D. Favrat, J. Schiffmann, J. Wegele. "Experimental investigation of a thermally driven heat pump based on a double organic Rankine cycle and an oil-free compressor-turbine unit." *Int. J. Refrig.* 44 (2014): 91-100. <https://doi.org/10.1016/j.ijrefrig.2014.04.024>
- [21] Iglesias, A. and D. Favrat. "Innovative isothermal oil-free co-rotating scroll compressor-expander for energy storage with first expander tests." *Energy Conserve. Manage.* 85 (2014): 565-572. <https://doi.org/10.1016/j.enconman.2014.05.106>
- [22] Mendoza, L.C., S. Lemofouet, J. Schiffmann. "Two-phase and oil-free co-rotating scroll compressor/expander." *Appl. Therm. Eng.* 148 (2019): 173-187. <https://doi.org/10.1016/j.applthermaleng.2018.11.037>
- [23] Dmitriev, O. and L.M. Arbon. "Comparison of energy-efficiency and size of portable oil-free screw and scroll compressors." *IOP Conf. Ser.: Mater. Sci. Eng.* 232 (2017): 012057. <https://doi.org/10.1088/1757-899X/232/1/012057>
- [24] Suamir, I.N., I.N.G. Baliarta, M.E. Arsana, I.P.S. Negara. "Condenser-evaporator approach temperatures and their influences on energy performance of water cooled chillers." *Proceeding of the 14th International Conference on QIR (Quality in Research)* (2015): 428-433.
- [25] Suamir, I.N., I.N.G. Baliarta, M.E. Arsana, I.W. Temaja. "The Role of condenser approach temperature on energy conservation of water cooled chiller." *Adv. Sci. Lett.* 23 (2017): 12202-12205. <https://doi.org/10.1166/asl.2017.10602>

- [26] Suamir, I.N., I.N.G. Baliarta, M.E. Arsana, Sudirman, I.M. Sugina. "Field-based analyses on approach temperatures for performance evaluation of centralized air conditioning system in a shopping mall building." *IOP Conf. Ser.: J. Physics* 1569 (2020): 032041. <https://doi.org/10.1088/1742-6596/1569/3/032041>
- [27] EN, BS. "Refrigerating Systems and Heat Pumps—Safety and Environmental Requirements." (2008).
- [28] Standard ASHRAE. "Designation and safety classification of refrigerants." *Ansi/Ashrae Standard* (2008): 34-2007.
- [29] IEEE Power Engineering Society. (2004). IEEE standard test procedure for polyphase induction motors and generators. *ANSI, IEEE Standard 112-B*.
- [30] Yu, Jianfeng, Ting Zhang, and Jianming Qian. *Electrical Motor Products: International Energy-Efficiency Standards and Testing Methods*. Elsevier, 2011. <https://doi.org/10.1533/9780857093813>
- [31] Hamamatsu, T., T. Iwatsubo, and M. Saikawa. "Development of advanced heat pumps for room cooling, heating and hot water supplying." In *Heat Pumps*, pp. 477-486. Pergamon, 1990. <https://doi.org/10.1016/B978-0-08-040193-5.50057-2>.
- [32] Rosen, M.A. and B.V. Reddy. "Chapter 7 - High Efficiency Plants and Building Integrated Renewable Energy Systems. Handbook of Energy Efficiency in Buildings a Life Cycle Approach", (2019): 441-595. <https://doi.org/10.1016/B978-0-12-812817-6.00040-1>.